Available online at www.jbr-pub.org.cn

Open Access at PubMed Central

The Journal of Biomedical Research, 2020 34(4): 309–317

JBR

Original Article

Improved image resolution on thoracic carcinomas by quantitative ^{18}F-FDG coincidence SPECT/CT in comparison to ^{18}F-FDG PET/CT

Yuming Zheng[1], Chaoling Jin[1], Huijuan Cui[2], Haojie Dai[3], Jue Yan[1], Pingping Han[1,△,✉], Bailing Hsu[4,△,✉]

[1]Nuclear Medicine Department, [2]Oncology of Integrative Medicine Department, China-Japan Friendship Hospital, Beijing 100029, China;
[3]Nuclear Medicine Department, Danli Hospital, Beijing 100073, China;
[4]Nuclear Science and Engineering Institute, University of Missouri-Columbia, Columbia, MO 65201, USA.

Abstract

Currently, ^{18}F-FDG coincidence SPECT (Co-SPECT)/CT scan still serves as an important tool for diagnosis, staging, and evaluation of cancer treatment in developing countries. We implemented full physical corrections (FPC) to Co-SPECT (quantitative Co-SPECT) to improve the image resolution and contrast along with the capability for image quantitation. FPC included attenuation, scatter, resolution recovery, and noise reduction. A standard NEMA phantom filled with 10:1 F-18 activity concentration ratio in spheres and background was utilized to evaluate image performance. Subsequently, 15 patients with histologically confirmed thoracic carcinomas were included to undergo a ^{18}F-FDG Co-SPECT/CT scan followed by a ^{18}F-FDG PET/CT scan. Functional parameters as SUVmax, SUVmean, SULpeak, and MTV from both quantitative Co-SPECT and PET were analyzed. Image resolution of Co-SPECT for NEMA phantom was improved to reveal the smallest sphere from a diameter of 28 mm to 22 mm (17 mm for PET). The image contrast was enhanced from 1.7 to 6.32 (6.69 for PET) with slightly degraded uniformity in background (3.1% *vs.* 6.7%) (5.6% for PET). Patients' SUVmax, SUVmean, SULpeak, and MTV measured from quantitative Co-SPECT were overall highly correlated with those from PET (r=0.82–0.88). Adjustment of the threshold of SUVmax and SUV to determine SUVmean and MTV did not further change the correlations with PET (r=0.81–0.88). Adding full physical corrections to Co-SPECT images can significantly improve image resolution and contrast to reveal smaller tumor lesions along with the capability to quantify functional parameters like PET/CT.

Keywords: ^{18}F-FDG, coincidence SPECT/CT, full physical corrections, thoracic carcinomas, image quantitation

△These authors contributed equally to this work.

✉Corresponding authors: Pingping Han, Nuclear Medicine Department, China-Japan Friendship Hospital, Beijing 100029, China. Tel: +86-010-84205508, E-mail: hanjiangpingping@163.com; Bailing Hsu, Nuclear Science and Engineering Institute, University of Missouri-Columbia, Columbia, MO 65201, USA. Tel: +1-573-882-8201, E-mail: bailinghsu@gmail.com.

Received 04 January 2019, Revised 21 May 2019, Accepted 04 June 2019, Epub 16 August 2019

CLC number: R445, Document code: A

The authors reported no conflict of interests.

https://doi.org/10.7555/JBR.33.20190004

Introduction

^{18}F-FDG (FDG) positron emission tomography/computed tomography (PET/CT) has been worldwide utilized as an important clinical tool in diagnosis, staging and treatment evaluation of various cancer schemes[1–2]. It has been reported that adding quantitative assessment for in FDG PET/CT scans to monitor the response of first-line chemotherapy can improve the prognostic value for lymphomas, breast cancer, non-small lung cancer, colorectal cancer and esophangel cancer[3]. In the historical pathway, single photon emission computed tomography (SPECT) and SPECT/CT systems with the capability of coincidence detection (Co-SPECT and Co-SPECT/CT) were introduced for local or whole-body tumor scan with FDG tracer. The role of FDG Co-SPECT/CT scan mainly has been addressed by the simple technology and its cost-effectiveness fitted in the sequence of tumor management[4–6]. Nowadays, FDG Co-SPECT/CT scan still serves as an important clinical tool to receive medical reimbursement in developing countries (*e.g.* China)[7–8]. Over the evolution for two decades, the annual usage of FDG Co-SPECT/CT scans remains enlarged although the number of private medical payment for FDG PET/CT scans continuously increases in recent years. Nevertheless, FDG Co-SPECT/CT scan traditionally does not contain the capability of quantitative assessment and further clinical expansion for the purpose of improved diagnosis, staging, and treatment evaluation like FDG PET/CT scan is highly restricted[9]. In this study, we implemented full physical corrections to eliminate the physical interference in FDG Co-SPECT/CT scan allowing to enhance the detection of small lesions and simultaneously enabling the quantitative assessment of tumor characteristics. Both phantom and a group of patients with histologically confirmed thoracic carcinomas were utilized to evaluate the image performance of quantitative Co-SPECT compared to conventional (non-quantitative) Co-SPECT and PET. The evaluation of image quantitation of FDG Co-SPECT/CT scans included to utilize standardized uptake value (SUV) and metabolic tumor volume (MTV) using FDG PET/CT scans as the reference standard.

Materials and methods

Phantom study

A series of 17 point sources with an activity of 185.3 kBq ± 5% and aligned in a geometry of a cross shape with a separate distance of 40.0 mm apart were utilized to measure the image resolution of reconstructed images. An International Electrotechnical Commission (IEC) 61675-1 emission phantom (NEMA phantom) consist of the shape of an upper human body and 6 hollow glass spheres (inner diameters 37, 28, 22, 17, 13, and 10 mm) was employed to measure the image contrast and uniformity of reconstructed images. The background volume of the NEMA phantom and the 6 spheres were filled with ^{18}F-FDG mixed with pure water using a roughly 10:1 sphere-to-background activity concentration ratio. The initial tracer activity concentration was specifically calibrated to the start of the measurement: 15.1 kBq/mL ± 1% in the phantom background and 168.6 kBq/mL ± 5% in the 6 small spheres.

Patient study

The prospective patient study consisted of 61 tumor lesions from 15 patients [13 males and 2 females; aged 46−79 years old, with a mean age of (62.5±8.8) years] whose thoracic carcinomas were histologically confirmed between July 2014 and August 2015 (10 lung cancers, 2 lung cancers accompanied with gastric cancer, 1 thymic carcinoma, 1 pleural mesothelioma, 1 esophagus cancer). Patient characteristic and pathological diagnosis of tumor lesions are listed in ***Table 1***. All patients underwent both thoracic ^{18}F-FDG Co-SPECT/CT and ^{18}F-FDG PET/CT scans. This study adopted the standard protocol to require patient fasting and resting for at least 6 hours that ensured <8.3 mmol/L blood sugar level prior to the intravenous administration of FDG. For each patient, FDG dose was determined by a weight formula (3.7 MBq/kg body weight). Forty minutes post the FDG injection, the Co-SPECT/CT scan was started, and upon the completion of scan, the PET/CT scan was intermediately followed. Each patient signed the informed consent form approved by the medical ethics committee of China-Japan Friendship Hospital.

^{18}F-FDG Co-SPECT/CT imaging

^{18}F-FDG Co-SPECT/CT scan was performed on a GE Hawkeye Infinia SPECT/CT scanner (GE Healthcare, USA) equipped with two 2.54 cm NaI (Tl) crystals, ultra-fast coincidence detection system (CoDe8 VARICAM circuitry) and lead-tin-copper septa for 2D 511-keV coincidence data acquisition. An integrated low-dose CT system was integrated for patient positioning and attenuation correction. Prior to the Co-SPECT acquisition, a topogram was acquired for patient positioning. The coincidence emission data

Table 1 **Patient characteristics and pathological diagnosis of tumor lesions**

Patients	Gender	Age (year)	Height (cm)	Weight (kg)	No. of tumor lesions	Pathological diagnosis
1	Male	57	175	65	1	Esophagus cancer
2	Male	60	160	61	4	Thymic carcinoma
3	Male	71	171	67	1	Lung adenosquamous carcinoma
4	Male	68	168	85	3	Lung squamous carcinoma
5	Male	79	176	72	8	Lung adenocarcinoma
6	Male	58	164	75	3	Lung adenocarcinoma
7	Male	69	170	71	6	Lung adenocarcinoma
8	Female	51	165	55	3	Lung adenocarcinoma
9	Male	65	171	65	2	Lung adenocarcinoma
10	Male	61	170	55	8	Lung adenocarcinoma and gastric cancer
11	Male	63	160	53	6	Gastric cancer
12	Male	69	178	55	1	Lung squamous carcinoma
13	Male	46	168	78	10	Pleural mesothelioma
14	Female	69	160	69	3	Lung adenocarcinoma
15	Male	52	180	90	2	Lung adenocarcinoma

was acquired with the setting of 12-degree axial acceptance, 128×128 matrix, 4.0 mm pixel size, 460–562 keV energy window, 64 projections within 360-degree continuous and repetitive rotations for total 30 minutes scan time. The CT transmission data was acquired with 140 kVp and 2.5 mA for 10 minutes. Conventional Co-SPECT images with CT attenuation correction were reconstructed by the vendor provided system implementing ordered subsets expectation maximization (OSEM) (20 iterations and 2 subsets) and intermediate Gauss filter every 4 iterations. Quantitative Co-SPECT images were reconstructed by a separated software AllSUVQ (China) utilizing OSEM (5 iterations and 8 subsets) with CT attenuation correction, resolution recovery with specially-dependent point spread functions (PSF), scatter correction with the model-based method and reconstruction-based nose filter to correct for physical interference in images[10–14]. For quantitative Co-SPECT images, pixel intensity was converted to a physical unit (Bq/mL) using a conversion factor obtained from a separated study with a uniform phantom.

^{18}F-FDG PET/CT imaging

^{18}F-FDG PET/CT scan was performed on a GE Discovery Elite (690) PET/CT scanner (GE Healthcare). Prior to PET imaging, a low-dose CT scan was acquired craniocaudally during shallow breathing. Effective tube current was 80 mA, tube voltage of 140 kV and care dose switched on. Slice thickness was 3.75 mm, and bed speed was 39.37 mm/s with pitch of 0.984. PET imaging was performed in 3D mode with time of flight (TOF) as 2.5 minutes per bed position at an axial sampling thickness of 3.25 mm per slice and 15.7 cm field of view. The vendor provided PET image reconstruction utilizes coincidence events from a delayed coincidence window for random correction and a model-based approach for scatter correction. 3D TOF PET images were reconstructed with OSEM (24 subsets and 2 iterations), filter cut-off 6.4 mm and the PSF with enhanced image resolution.

Image analysis

For the study of point sources aligned in a cross shape, image resolution was assessed by the full width at half maximum (FWHM) of each point in in-plane and axial directions[15]. For the study of NEMA phantom, image contrast was defined as (the intensity of largest sphere-background activity) background activity. Image uniformity was calculated by (SD/mean) in background area using a region of interest (ROI) with 25 mL. To evaluate the quantitative accuracy for measurement of F-18 activity concentrations in 6 spheres, measured values were compared to the corresponded true values in quantitative Co-SPECT and PET images. Accuracy curves as functions of diameters were plotted to depict the impact of partial volume effect (PVE) for

decreased diameters. Additionally, mean activity concentration in background area was also measured to assess the accuracy without PVE. For the patient study, analysis of metabolic uptake in ^{18}F-FDG-avid tumor lesions for quantitative Co-SPECT and PET images was accomplished in a dedicated reporting workstation (MedEx, China) to measure the maximum and mean standardized uptake values (SUVmax and SUVmean), peak lean body mass SUV (SULpeak) and metabolic tumor volume (MTV) in the lesions of interest. By definition, SUVmax is the highest value of SUV within a ROI. The SUVmean is the average value of SUV within the region of interest with the default threshold as 40% SUVmax. The SULpeak is the averaged SUV in a spherical ROI with 1.0 mL centering around the hottest point in the tumor foci corrected for lean body mass. MTV is the volume of the tumor lesion with the default threshold above 2.5 SUV. Further analysis for SUVmean and MTV obtained from quantitative Co-SPECT against PET was also performed to verify the stability of measurement under various levels of threshold values as 30%–50% SUVmax for SUVmean and 2.8 –40 SUV for MTV.

Statistical analysis

For the patient study, difference of functional parameters (SUVmax, SUVmean, SULpeak and MTV) from quantitative Co-SPECT and PET were verified by paired *t*-test. A $P<0.05$ was considered significant. Using functional parameters from PET images as the reference standard, linear regression was performed to obtain the correlation of functional parameters form quantitative Co-SPECT with PET images. All the statistical data analysis was performed with a commercialized software (GraphPad Prism V5.0, USA).

Results

Phantom study

Performance of conventional Co-SPECT, quantitative Co-SPECT and PET for a series of line sources and NEMA phantom were listed in ***Table 2*** with corresponded images shown in ***Fig. 1*** and ***Fig. 2***. With full physical corrections, mean image resolution of Co-SPECT was improved from (13.1±1.2) mm to (9.5±0.8) mm in the in-plane direction and from (13.5±1.1) mm to (9.8±0.7) mm in the axial direction. The image contrast was enhanced from 1.79 to 6.32. As a tradeoff, the image uniformity in background area were slightly degraded from 3.1% to 6.7%. For PET images, the in-plane image resolution was (7.4±0.4) mm and (7.6±0.5) mm for the axial direction. The image uniformity was 5.6%. ***Fig. 3*** demonstrates the accuracy curves of quantitative Co-SPECT and PET images to measure the activity concentration as functions of sphere diameters.

Table 2 **Parametric performance of Co-SPECT and PET images for NEMA phantom**

Image parameters	Conventional Co-SPECT	Quantitative Co-SPECT	PET
In-plane image resolution (mm)	*,+13.1±1.2	&9.5±0.8	7.4±0.4
Axial image resolution (mm)	*,+13.5±1.1	&9.8±0.7	7.6±0.5
Image contrast	*,+1.79	6.32	6.69
Image uniformity	*,+3.1%	6.7%	5.6%

*significant difference between conventional Co-SPECT and quantitative Co-SPECT ($P<0.05$); +significant difference between conventional Co-SPECT and PET; &significant difference between quantitative Co-SPECT and PET ($P<0.05$).

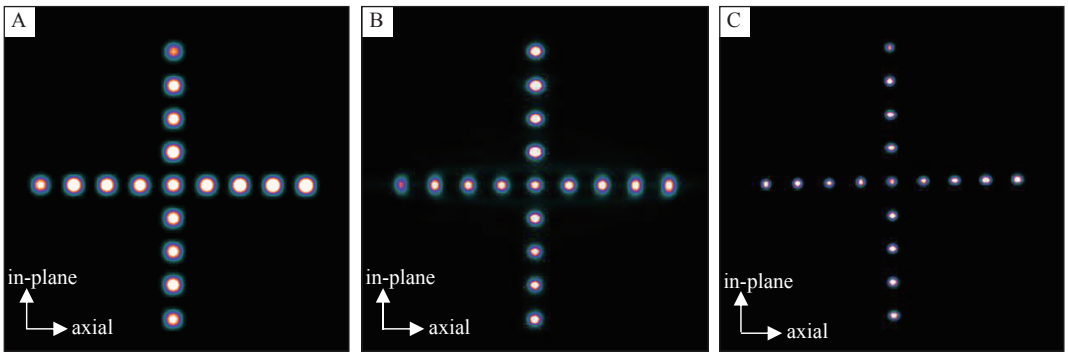

Fig. 1 **Images of point sources aligned in a cross shape.** A: conventional Co-SPECT; B: quantitative Co-SPECT; C: PET.

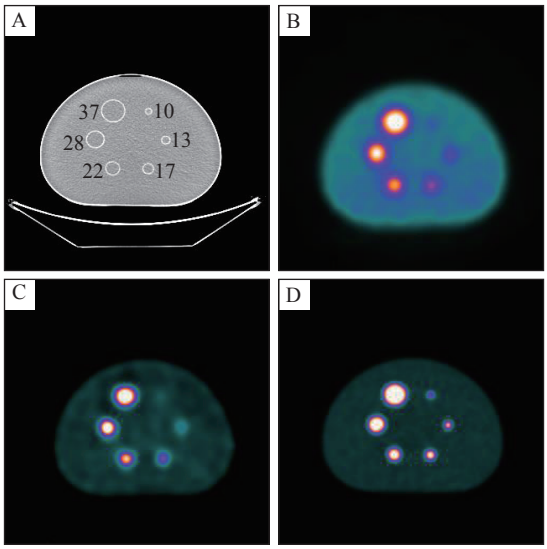

Fig. 2 **NEMA phantom images.** A: CT with numbers indicating diameters of spheres in mm; B: conventional Co-SPECT; C: quantitative Co-SPECT; D: PET.

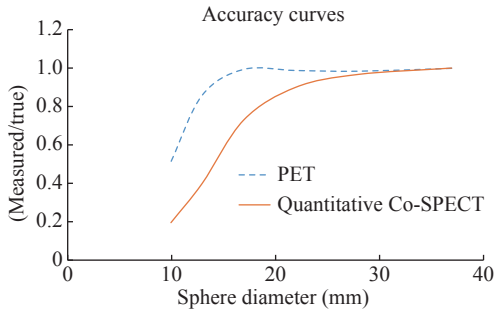

Fig. 3 **Accuracy curves of quantitative Co-SPECT and PET as functions of sphere diameters.**

Among spheres with diameters ≥28 mm, the accuracy to measure F-18 activity concentration for quantitative Co-SPECT was >97.1% and gradually declined when smaller diameters decreased due to increased PVE. For PET, the >98.5% accuracy was observed for spheres with diameters ≥17 mm. In the background area of NEMA phantom without PVE, both quantitative SPECT and PET demonstrated >99% accuracy.

Patient study

Fig. 4 represents conventional Co-SPECT, quantitative Co-SPECT and PET images of a patient with histologically confirmed lung adenocarcinoma. From visual assessment, quantitative Co-SPECT outperformed conventional Co-SPECT mainly with higher image resolution and contrast moving closer to PET. Among 15 patients and 61 tumor lesions, functional parameters of quantitative Co-SPECT were significantly different from those of PET. Mean

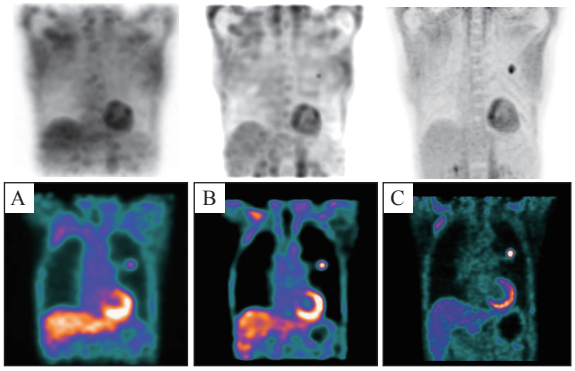

Fig. 4 **Representative images from a patient with histologically confirmed lung adenocarcinoma in maximum intensity projection and coronal view.** A: conventional Co-SPECT; B: quantitative Co-SPECT; C: PET images.

difference of SUVmax as (Co-SPECT-PET) was –1.822 g/mL, and (–1.250 g/mL, –1.808 g/mL, 34.97 mL) for SUVmean, SULpeak and MTV (all P<0.0025). Nonetheless, linear regression of SUVmax revealed strong correlation and close to unity slope for quantitative Co-SPECT and PET as r=0.8218 (95% CI, 0.7186–0.8895) and y=1.0804x−2.7765 (***Fig. 5***). Linear regression for SUVmean and SULpeak demonstrated similar findings as r=0.8390 (95% CI, 0.7444–0.9005) and y=1.0601x−1.679, and r=0.8171 (95% CI, 0.7116 –0.8865) and y=0.9736x−1.5318, respectively. For the MTV measurement, the correlation between quantitative Co-SPECT and PET remained strong as r=0.8791 (95% CI, 0.8056–0.9260), but relatively increased slope and offset as y=1.2021x+20.037. In the verification of measurement tendency for SUVmean by testing the threshold of 30%~50% SUVmax, correlations with PET stayed similar (r=0.8315–0.8413) ***(Fig. 6)***. The range of slope and offset in linear regression were (0.893–1.2197) and (−1.3276–−2.0431) (g/mL). In the verification of measurement tendency for MTV by testing the threshold of 2.8–4.0 SUV, the threshold of 2.8 SUV showed the highest correlation (r=0.8779) ***(Fig. 7)***. The slope and offset in linear regression were 1.0198 and 16.746 (mL).

Discussion

In this research work, we implemented full physical corrections to Co-SPECT (quantitative Co-SPECT) and observed improved image resolution and contrast in both NEMA phantom and patient images. Methods for physical corrections are comparable to previously reported methods for PET and PET/CT imaging[10–14]. In the NEMA phantom study, the improved image resolution in quantitative Co-SPECT enabled to depict

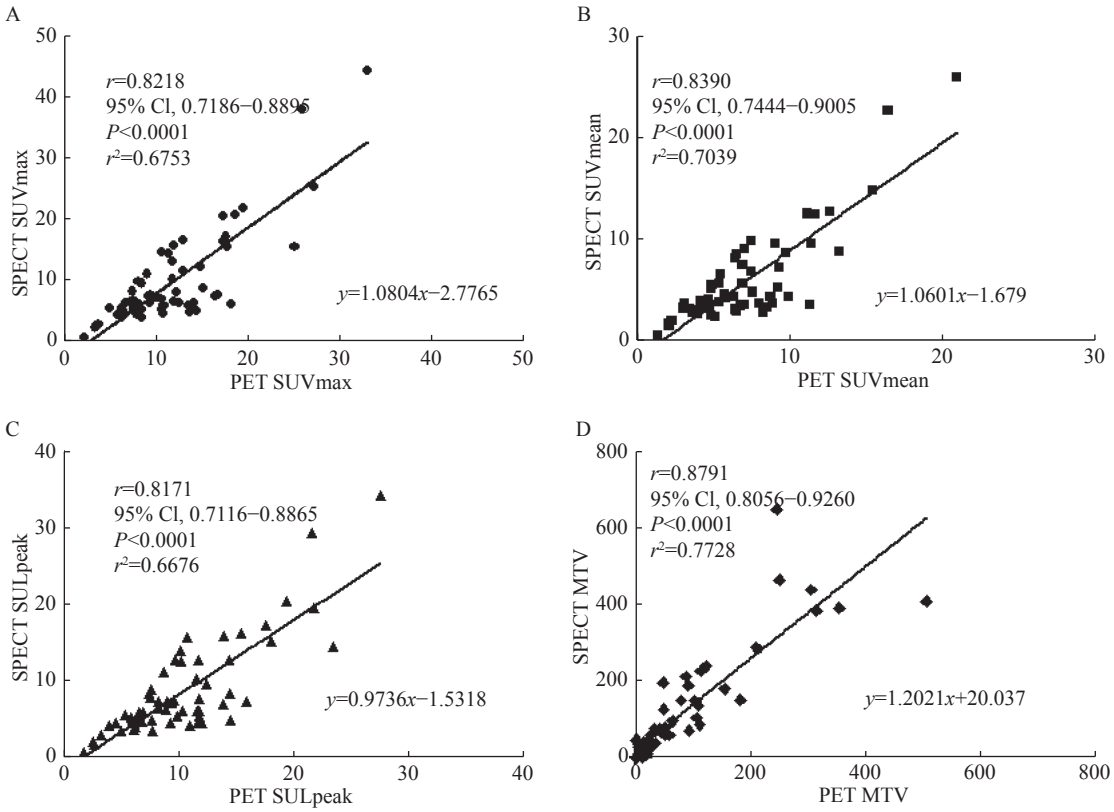

Fig. 5 **Linear regression for SUVmax, SUVmean, SULpeak and MTV obtained from quantitative Co-SPECT and compared to those of PET.** A: SUVmax; B: SUVmean; C: SULpeak; D: MTV.

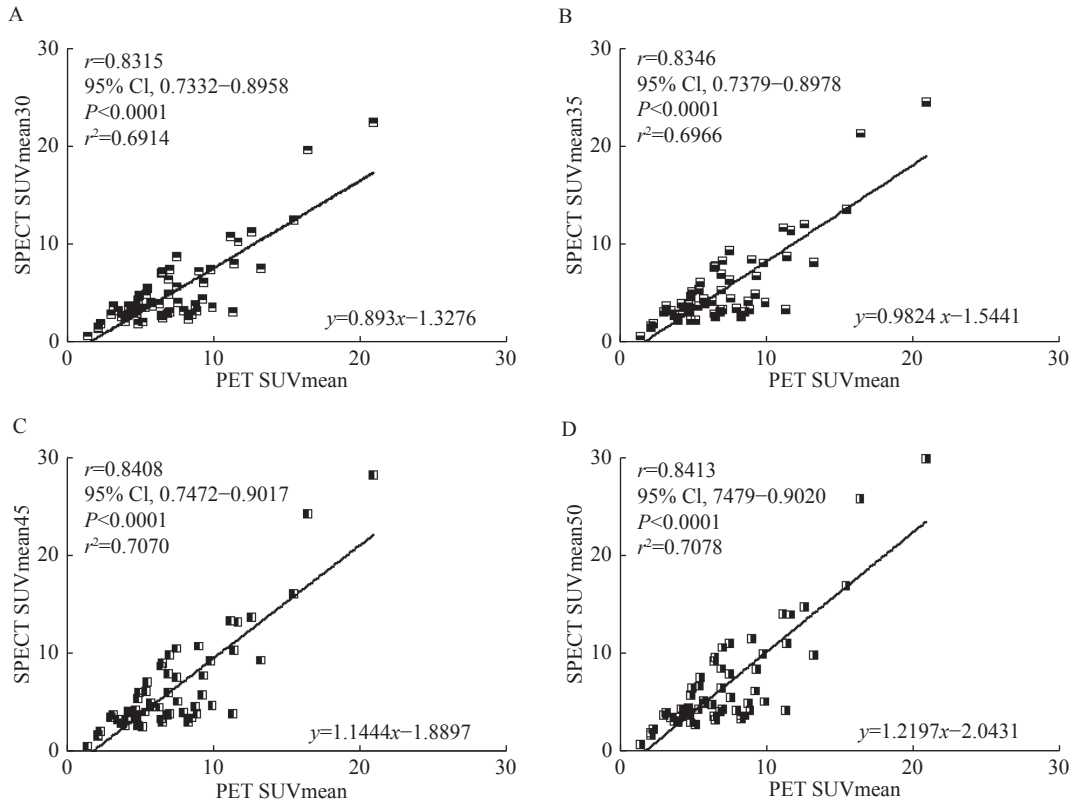

Fig. 6 **Linear regression for SUVmean obtained from quantitative Co-SPECT with different thresholds of % SUVmax (30%–50%) compared to those of PET.** A: 30% threshold; B: 35% threshold; C: 45% threshold; D: 50% threshold.

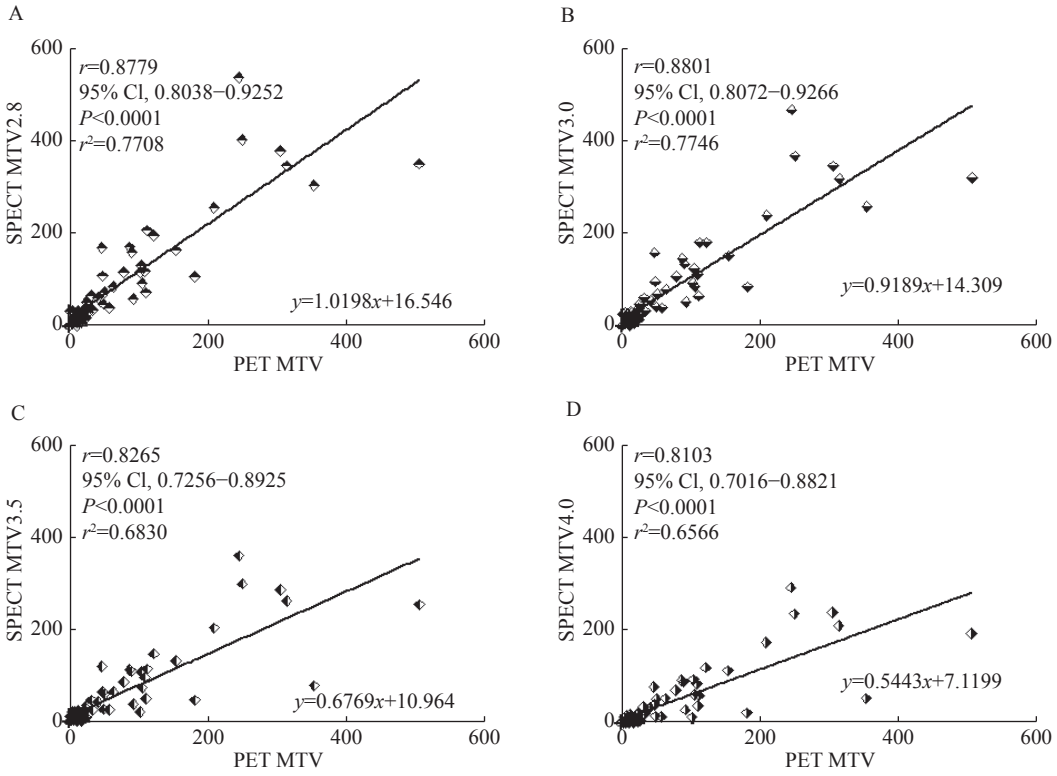

Fig. 7 **Linear regression for MTV obtained from quantitative Co-SPECT with different thresholds of SUV (2.8–4.0) compared to those of PET.** A: 2.8 threshold; B: 3.0 threshold; C: 3.5 threshold; D: 4.0 threshold.

smaller sphere (diameter=2.2 mm) than conventional Co-SPECT (diameter=2.8 mm). The enhanced image contrast (1.79 to 6.32) allowed more clear distinction of small spheres relative to background than conventional Co-SPECT. These improvements were mainly attributed to the contribution of scatter and resolution recovery as similar effects were also observed in PET studies[10–13]. Furthermore, we found that the image uniformity of quantitative Co-SPECT was slightly lower (6.7%) than that of conventional Co-SPECT (3.1%). This was the coeffect of resolution recovery to slightly elevate image noise as the tradeoff[13]. Nonetheless, slight degradation of image uniformity mainly occurred in background area and generally should not impact on image interpretation since tumor uptake usually appeared in hot spot. Another merit of quantitative Co-SPECT was the capability for quantitative measurement of F-18 activity concentration in unit of Bq/mL that provided the requisite to quantify functional parameters such as SUV and MTV in patient images. In the patient study, we verified the accuracy of functional parameters measured from quantitative Co-SPECT against PET as the reference standard. As resulted, SUVmax, SUVmean, SULpeak and MTV from quantitative Co-SPECT images were overall strongly correlated with those of PET images (r=0.8171 –0.8791). Further adjustment of the threshold in the range of 30%–50% SUVmax for determination of SUVmean didn't significantly modify correlation (r=0.8315 –0.8413). Adjustment of the threshold in the range of 2.8 – 4.0 SUV for determination of MTV reported the best correlation in 3.0 SUV (r=0.8801) and not significantly different from other thresholds (r=0.8103 –0.8779). Consequently, measurements of SUVmean and MTV with thresholds in tested ranges were relatively stable for quantitative Co-SPECT.

In the clinical setting, conventional Co-SPECT images in FDG Co-SPECT/CT scan were reconstructed by the vendor provided program for the clinical purpose of diagnosis, staging and treatment evaluation. Under limited image resolution and contrast, it is highly possible that small tumors may often hide to give incorrect diagnosis. ***Fig. 8*** demonstrates a representative patient with a metastatic mediastinal lymph node as esophagus cancer near myocardium. In conventional Co-SPECT images, the tumor in left lung was missing and uncovered in both quantitative Co-SPECT (MTV=4.18 mL) and PET images (MTV=3.93 mL). Consequently, full physical corrections in FDG Co-SPECT/CT scan can improve the sensitivity of tumor detection and image quantitation that would encompass high potentials toward clinical utilization like FDG PET/CT scan.

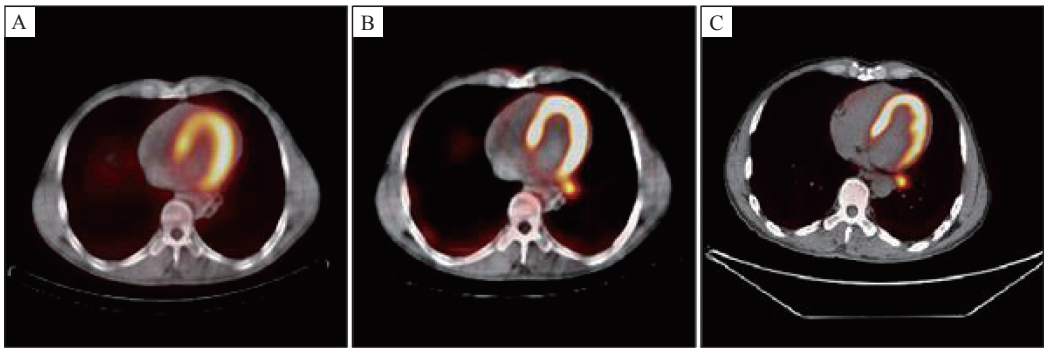

Fig. 8 **A representative patient with a metastatic mediastinal lymph node as esophagus cancer near myocardium.** A: conventional Co-SPECT; B: quantitative Co-SPECT; C: PET.

It has been well known that the design of Co-SPECT/CT scanner with NaI (Tl) crystal, 2D septa, relatively slow electronics and two flat detectors for rotatory acquisition encompasses large gap in hardware performance compared to the most high-end PET/CT scanner with lutetium-based crystal, 3D acquisition without septa, fast electronics for time of flight and full ring detectors[16–20]. Due to large limitation in hardware design, the performance of Co-SPECT was inferior to PET by less statistical counts and lower spatial resolution. This hardware limitation can be significantly improved by full physical corrections as shown in both phantom and patient images. To our knowledge, this is the first study reporting the quantitation of Co-SPECT utilizing PET as the reference standard. While Co-SPECT/CT scanners still serve as a clinical utility in developing countries, the enhancement in image spatial resolution and contrast with quantitative capability by full physical corrections would provide a practical solution to improve the current performance toward the standard of PET/CT.

In this study, due to the concern of radiation dose by two FDG injections, we specifically designed to image a patient twice using a single FDG injection to complete a FDG Co-SPECT/CT scan followed by a FDG PET/CT scan. The time point to start FDG Co-SPECT/CT scan was 40 minutes post FDG injection, and time gap to start these two scans was usually 50 minutes. In general, the standard protocol adopted 60 minutes to the scan post FDG injection. Whether the FDG uptake in tumors may alter due to delayed scan time cannot be further verified in our study. Nonetheless, strong correlations of functional parameters obtained from FDG Co-SPECT/CT and PET/CT scan were observed in our study. This study only included small number of patients, and the majority of tumors were lung adenocarcinoma. Future studies should extend the patient sample sizes as well as testing on various types of tumors to warrant the approach of quantitative quantitative F-FDG Coincidence SPECT/CT.

Conventional FDG Co-SPECT/CT scan had relatively low image resolution and contrast. Adding full physical corrections to Co-SPECT images can significantly improve image resolution and contrast to reveal smaller tumor lesions along with the capability to quantify functional parameters like PET/CT.

Acknowledgments

This research study was supported by the internal research grant from China-Japan Friendship Hospital, Beijing, China (Grant No. 2016-1QN-9)

References

[1] Facey K, Bradbury I, Laking G, et al. Overview of the clinical effectiveness of positron emission tomography imaging in selected cancers[J]. *Health Technol Assess,* 2007, 44(11): iii-iv, xi–267.

[2] Gallamini A, Zwarthoed C, Borra A. Positron emission tomography (PET) in oncology[J]. *Cancers,* 2014, 6(4): 1821–1889.

[3] Ben-Haim S, Ell P. ^{18}F-FDG PET and PET/CT in the evaluation of cancer treatment response[J]. *J Nucl Med,* 2009, 50(1): 88–99.

[4] Martin WH, Delbeke D, Patton JA, et al. FDG-SPECT: correlation with FDG-PET[J]. *J Nucl Med,* 1995, 36(6): 988–995.

[5] Martin WH, Delbeke D, Patton JA, et al. Detection of malignancies with SPECT versus PET, with 2-[fluorine-18] fluoro-2-deoxy-D-glucose[J]. *Radiology,* 1996, 198(1): 225–231.

[6] Delbeke D, Patton JA, Martin WH, et al. FDG PET and dual-head gamma camera positron coincidence detection imaging of suspected malignancies and brain disorders[J]. *J Nucl Med,* 1999, 40(1): 110–117.

[7] Qiao WL, Zhao JH, Wang C, et al. Comparison of ^{18}F-FDG

coincidence SPECT imaging and computed tomography in the initial staging and therapeutic evaluation of lymphomas[J]. *Chin J Oncol (in Chinese),* 2007, 29(7): 536–539.

[8] Mao YS, He J, Zheng R, et al. The role of ^{18}F-FDG DHC SPECT-CT in the diagnosis and staging for lung cancer[J]. *Chin J Oncol (in Chinese),* 2008, 30(12): 933–936.

[9] Seo Y, Mari C, Hasegawa BH. Technological development and advances in single-photon emission computed tomography/computed tomography[J]. *Semin Nucl Med,* 2008, 38(3): 177–198.

[10] Barret O, Carpenter TA, Clark JC, et al. Monte Carlo simulation and scatter correction of the GE Advance PET scanner with SimSET and Geant4[J]. *Phys Med Biol,* 2005, 50(20): 4823–4840.

[11] Watson PG, Mainegra-Hing E, Tomic N, et al. Implementation of an efficient Monte Carlo calculation for CBCT scatter correction: phantom study[J]. *J Appl Clin Med Phys,* 2015, 16(4): 216–227.

[12] Sureau FC, Reader AJ, Comtat C, et al. Impact of image-space resolution modeling for studies with the high-resolution research tomograph[J]. *J Nucl Med,* 2008, 49(6): 1000–1008.

[13] Rahmim A, Qi JY, Sossi V. Resolution modeling in PET imaging: theory, practice, benefits, and pitfalls[J]. *Med Phys,* 2013, 40(6): 064301.

[14] Hsu B, Hu LH, Yang BH, et al. SPECT myocardial blood flow quantitation toward clinical use: a comparative study with ^{13}N-Ammonia PET myocardial blood flow quantitation[J]. *Eur J Nucl Med Mol Imaging,* 2017, 44(1): 117–128.

[15] Gong K, Cherry SR, Qi JY. On the assessment of spatial resolution of PET systems with iterative image reconstruction[J]. *Phys Med Biol,* 2016, 61(5): N193–N202.

[16] Melcher CL. Scintillation crystals for PET[J]. *J Nucl Med,* 2000, 41(6): 1051–1055.

[17] Bettinardi V, Mancosu P, Danna M, et al. Two-dimensional vs three-dimensional imaging in whole body oncologic PET/CT: a Discovery-STE phantom and patient study[J]. *Q J Nucl Med Mol Imaging,* 2007, 51(3): 214–223.

[18] Tanaka E, Hasegawa T, Yamashita T, et al. A 2D/3D hybrid PET scanner with rotating partial slice-septa and its quantitative procedures[J]. *Phys Med Biol,* 2000, 45(10): 2821–2841.

[19] Surti S. Update on time-of-flight PET imaging[J]. *J Nucl Med,* 2015, 56(1): 98–105.

[20] El Fakhri G, Surti S, Trott CM, et al. Improvement in lesion detection with whole-body oncologic time-of-flight PET[J]. *J Nucl Med,* 2011, 52(3): 347–353.